CHALMERS
UNIVERSITY OF TECHNOLOGY

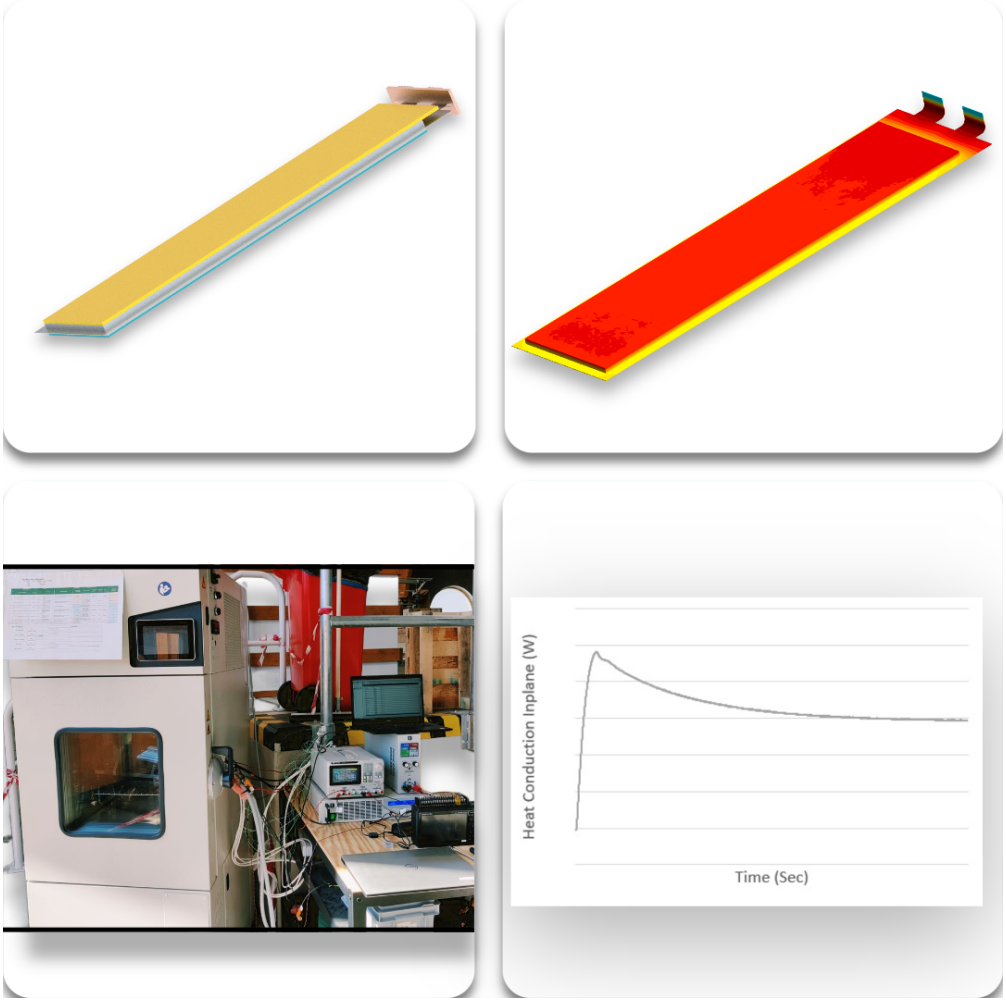

Thermal management for electric aviation

A product development approach

Master's thesis in Product Development

Uppili Murali

DEPARTMENT OF MECHANICS AND MARITIME SCIENCES
CHALMERS UNIVERSITY OF TECHNOLOGY
Gothenburg, Sweden 2022
www.chalmers.se

Master's thesis 2022

Thermal management for electric aviation

A product development approach

Uppili Murali

CHALMERS
UNIVERSITY OF TECHNOLOGY

Department of Mechanics And Maritime Science
Division of Vehicle Engineering and Autonomous Systems
Chalmers University of Technology
Gothenburg, Sweden 2022

Thermal management for electric aviation
A product development approach
Uppili Murali

Supervisor: Oskar Lund and Hanna Wiggman, NorthVolt AB
Examiner: Prof. Simone Sebben, Division of Vehicle Engineering and Autonomous Systems, Chalmers University of Technology

Report Number: 2022:42

Master's Thesis 2022
Department of Mechanics And Maritime Science
Division of Vehicle Engineering and Autonomous Systems
Chalmers University of Technology
SE-412 96 Gothenburg
Telephone +46 31 772 1000

Cover: Cell with module components (Top Left), Temperature distribution of cell (Top Right), Picture of Test setup (Bottom Left) and Plots of Heat Conduction Vs Time (Bottom Right)

Typeset in LaTeX
Printed by Chalmers Reproservice
Gothenburg, Sweden 2022

Thermal management for electric aviation
A product development approach
Uppili Murali
Department of Mechanics and Maritime Sciences
Chalmers University of Technology

Abstract

Lithium-ion batteries (LIB's) are gaining momentum as a suitable and sustainable solution which can be utilised in many different applications and market. In order to be used in electric aircraft the batteries have to be lightweight, they also should also be safe enough to support second-line of defense during an electrical outage. As the global electric aircraft markets are expected to reach 27.7 billion USD by 2030. Battery industry is also expected to evolve and grow as the need evolves.

The safety, lifetime and reliability of LIBs are directly dependent on the operating cell temperature, which makes the thermal characterization of battery cells vital. Therefore, understanding the different thermal effects within the battery is of utmost importance for selecting the correct battery thermal management systems (BTMS). Understanding the heat distribution through the cell is important, as the cells exhibit orthotropic properties. This master thesis deals with understanding the dependence of different cooling strategies on the cell by creating a thermal model of a Li-ion pouch cell determining temperature distribution within the cell volume. A commercial CFD tool was utilised for performing the necessary simulations. The simulations were based on the heat generated during high discharge profiles. To validate the simulated results, experimental tests were conducted based on the predefined profiles and the results are will be utilized to further improve the simulation approach and calibrate the model to improve its accuracy and reliability.

It was observed that the thermal resistance is the highest only when the terminals are cooled and the lowest when the cells are cooled radially. The heating tests also showed similar trends in the thermal resistance characterisation. while comparing the experimental and simulated results the difference in maximum temperatures was found to be approximately 5%, with the experimental temperatures being higher than the simulated results. As the tests were carried out only on a specific discharge case while repeating the experiments for other discharge profiles might give a different perspective and more valuable information.

Keywords: Thermal management, CFD, electric aviation, experimental validation, cooling, heating

Acknowledgements

The thesis work has been carried out at the Division of Vehicle Engineering and Autonomous System, Department of Mechanics And Maritime Science at Chalmers Universty of Technology, Gothenburg Sweden and Northvolt AB, Stockholm, Sweden.

Firstly, I would like to express my sincere gratitude to my supervisors at NorthVolt AB, Oskar Lund and Hanna Wiggman, for their constant support, motivation and guiding me in the right direction during the course of this project. Their insightful knowledge and recommendations for the next steps to be taken in the project has proven to be extremely helpful to me. Another big thanks to Love Fältström, Kilian Menzl, Michel Chaupis, Tomas Muld and last but not the least Diego Buriti Thermal, Simulation and Testing experts at Northvolt for being our go-to persons in this thesis work.

I would also like to thank my examiner, Prof. Simone Sebben, for her valuable advice and for all the help when needed. Another sincere thanks to everyone at NorthVolt Battery Systems AB, for giving me the opportunity to work in such an encouraging, welcoming and diverse environment.

And finally, a big thanks to my parents, friends here in Sweden and back in India, who have always believed and encouraged me all these years. Their unconditional love and support is the reason for my success and enduring hardships thought out whole master's program.

Uppili Murali, Gothenburg, June 2022

List of Acronyms

Below is the list of acronyms that have been used throughout this thesis listed in alphabetical order:

LB	Lithium-ion Battery
LMA	Lithium Metal Anode
BES	Battery Energy Storage
TMS	Thermal Management System
BTMS	Battery Thermal Management System
BMS	Battery Management System
SoC	State of Charge
DoD	Depth of Discharge
OCV	Open circuit voltage
CFD	Computational Fluid Dynamics
CAD	Computer Aided Design
EV	Electric Vehicle
TIM	Thermal Interface Material

Contents

List of Acronyms **ix**

List of Figures **xiii**

List of Tables **xv**

1 Introduction **1**
1.1 Project Background . . . 1
1.2 Objective . . . 2
1.3 Delimitations . . . 2
1.4 Research Questions . . . 3
1.5 Report Outline . . . 3
1.6 Confidentiality . . . 3

2 Theory **5**
2.1 Heat Transfer Mechanisms . . . 5
2.1.1 Conduction . . . 5
2.1.2 Steady State and Transient Operation . . . 7
2.2 Li-ion Cells . . . 8
2.2.1 Lithium Metal Cells . . . 9
2.2.2 Cell Format . . . 9
2.2.3 Pouch Cell . . . 9
2.2.3.1 Cell construction . . . 9
2.2.4 Cell Terminologies . . . 11
2.2.5 Heat Generation . . . 12
2.2.6 Thermal Management . . . 14
2.2.6.1 Capacity fade: . . . 14
2.2.6.2 Thermal Runaway: . . . 14
2.2.7 Cooling Strategies . . . 14
2.2.7.1 Direct Cooling: . . . 14
2.2.7.2 Indirect Cooling: . . . 15
2.2.8 Heating . . . 15
2.2.8.1 Self-internal heating: . . . 16
2.2.8.2 Convective heating: . . . 16
2.2.8.3 Mutual pulse heating: . . . 16

3 Methodology **17**
3.1 Benchmarking . . . 17
3.2 Test cases . . . 18
3.3 Simulation Setup in Star CCM+ . . . 18
3.3.1 Cell Level Simulations . . . 18
3.3.1.1 Meshing . . . 18
3.3.1.2 Boundary Conditions . . . 18
3.3.2 Module Simulations . . . 20
3.3.2.1 Meshing . . . 20
3.3.2.2 Boundary Conditions . . . 21
3.4 Test Setup . . . 21
3.4.1 Compression Rig . . . 22
3.4.2 Calculation Methodology . . . 23

4 Results **27**
4.1 Cell Simulations . . . 27
4.1.1 Steady state . . . 27
4.1.2 Steady state Vs Transient . . . 28
4.1.3 Remarks . . . 29
4.2 Module Simulations . . . 29
4.2.1 Simulation Vs Experimental . . . 30
4.2.2 Heating . . . 31

5 Conclusion **33**
5.1 Future Work . . . 33

A Benchmarking **I**

List of Figures

1.1 Aviation market trends 1

2.1 Heat transfer through conduction 6
2.2 3D heat transfer by conduction 7
2.3 Li-ion cell 8
2.4 Comparison of Li-ion and Li-metal cells 9
2.5 Cell format 10
2.6 Pouch cell construction 10
2.7 Cell swelling 11
2.8 Heat generation Vs DoD 13
2.9 Dependence of internal resistance on the operating temperature and SOC 13
2.10 Immersion cooling 15
2.11 Corrugated channel from Tesla S 15

3.1 Thesis workflow 17
3.2 Geometry of the cell illustrating in plane and through plane axes . . . 19
3.3 Iso view of meshed cell 19
3.4 Section view of meshed cell 20
3.5 Module concept 20
3.6 Iso view of meshed module 21
3.7 Section view of meshed module 21
3.8 Schematic layout of test setup 22
3.9 Exploded view of test fixture 1 23
3.10 Exploded view of test fixture 2 24
3.11 Temperature measurement points on the cell 24
3.12 Temperature measurement points on the compression pad 25

List of Tables

2.1 Comparison of thermal & electrical parameters 5

4.1 Radial cooling Vs Long sided 27
4.2 Terminal cooling Vs Short side 28
4.3 Transient Vs Steady 29
4.4 Module Simulation 30
4.5 Simulation Vs Experimental 30
4.6 Experimental Heating 31

A.1 Benchmarking [19] I

1
Introduction

This chapter presents the reader with a background about Northvolt the need for batteries in the aviation industry, purpose of the thesis, research questions and delimitations.

1.1 Project Background

The rise of renewable power generation in the current energy market has created an increasing demands for different forms of energy storage systems. The lithium battery is at the forefront to fulfill the market demands of these storage systems, as they are lightweight with high energy density. Batteries which are intended to be used as an power source on an aircraft should have a high energy density, be lightweight, reliable, require minimal maintenance, and be able to operate efficiently in all sorts of harsh climates. As aviation standards continue to evolve and rise as the demand increases, there's a greater demand for the advancement of technology in the battery industry to deliver batteries capable to ensure the performance of the aircraft. Not only the batteries employed in the aircraft need to be lightweight, they also should be powerful enough to serve as the second-line of defense in the event of an electrical outage [1]. The Global electric aircraft markets are expected to reach 27.7 Billion USD by 2030 [2] as shown in Figure 1.1.

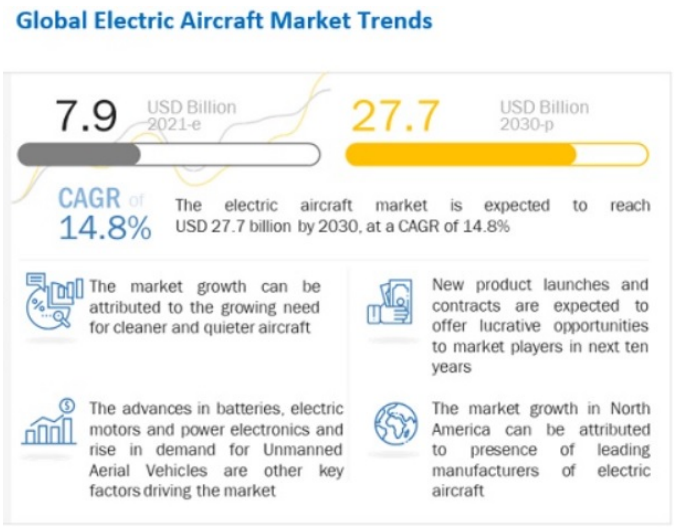

Figure 1.1: Aviation market trends[2]

The characteristics of Lithium batteries have made them attractive both for many different applications and sectors. However, despite their advantages, there are major hindrances pertaining to a battery system such as safety, cost, limited cycle life, etc. Temperature at which the Lithium batteries has to be operated have a high impact on safety, lifetime and performance. The optimum operating range for these batteries is 15-35°C [3] otherwise the performance and lifespan will be reduced and furthermore leading to undesirable events such as thermal runaway. In addition, temperature difference within the cells, battery modules within a battery pack should also be controlled, else it will impact its performance during operation and results in aging of the battery system. Thus, an effective battery thermal management system is necessary to dissipate the heat generated inside the battery system. In the case of low-temperature scenarios, heating of the battery cells is required to ensure its best performance [4].

1.2 Objective

The Objective of the thesis work is to

- To develop a 3-dimensional thermal model of a battery cell in a level where the geometry, anisotropic material properties are taken into consideration for different cooling strategies
- To use the above developed thermal model to estimate the battery cell temperature for predefined ambient conditions and cooling strategies.
- To develop a test setup to further investigate and validate the simulation results for different cooling strategies

1.3 Delimitations

As the thesis work is performed within 20 weeks and to achieve the goals within the stipulated time, there are various choices made in this thesis work to perform a detailed study. They are

- The numerical investigations and the experimental validations are based on the predefined conditions, other test conditions are not evaluated due to time constraint.
- Heat transfer by conduction will be considered, while radiation effects are not taken into account due to a relatively lower heat transfer.
- The experimental verification of internal temperatures within the battery cell is not carried out since it involves cell disassembly. However, surface temperatures which are estimated from the simulation model are compared with experimental results.
- No detailed CFD simulations of the cooling system will be performed.
- Battery cell aging and cell swelling is a complex function of drive cycles. Hence, they are ignored in this study

1.4 Research Questions

The work carried out during the thesis time period sought answers for the following research questions within the scope of the project.

1. What are the different strategies to cool and heat the cell for the predefined test conditions?

2. Which is the most effective position for cooling and heating the cell?

3. What could be the amount of heat flux that is necessary to removed or given into the cell in order to maintain the cell at the optimum temperature range?

1.5 Report Outline

This report begins with a brief introduction of the thesis work as well as the basic theory for the reader to be able to understand the work carried out. The report is then presented in chronological order of how the work was carried out, beginning with benchmarking and literature study, concept design along with conclusions. Potential future work and Recommendations given to the company are given at the end of the report.

1.6 Confidentiality

The data and information utilized in this thesis work are kept confidential and such confidential information shared by the participants are respected and not shared outside the research group. The anonymity of the research data are respected by not mentioning the organisation and personal information. The report uses data and facts from external references which are cited accordingly to acknowledge the work.

2
Theory

In this chapter, a brief explanation of the theoretical background necessary to understand the thesis work is laid out. It starts from the basics of heat transfer then moving into the different aspects of battery cells and finally briefly describes about the contemporary thermal management system.

2.1 Heat Transfer Mechanisms

Heat energy is one of the most useful forms of energy as it can be transferred one medium to another medium by different possible ways. They can also be transferred with or without the availability of transfer media. The heat energy always flows from a region which is at a higher temperature to lower temperature which is analogical to flow of electricity from higher potential region to lower potential region as comparted in Table 2.1. The primary way for heat transfer within the Li-ion cells is through conduction as the cell is made up of different solid materials and the heat transfer from the cell surface to the coolant takes place through convection either through direct or indirect means. The heat transfer through radiation are relatively very low as the temperature difference between the cell and the ambient temperature very small. It is necessary to consider heat losses through radiation only when the difference between source and sink is around 300°C [5]. Hence heat loss through radiation is excluded from this study.

Table 2.1: Comparison of thermal & electrical parameters [5]

	Thermal	Electrical
Flow	Heat	Current
Resistance	Thermal Resistance	Resistance
Potential	Temperature	Voltage

2.1.1 Conduction

When the heat is transferred within solids and also between solids which are in physical contact. When the heat energy is applied to a solid, the molecules which are constituted within the solids starts to vibrate with higher amplitudes and frequencies as they absorb the applied energy. Heat transfer through conduction is dependent on the thermal conductivity of the material k, the temperature difference between region of interests and the cross-sectional area perpendicular to the heat flow. In

the Figure 2.1 the heat flow Q through a solid with thermal conductivity k with one end of the solid at temperature T1 which is continuously heated and T2 is the temperature at a distance of δ x from T1. From Fourier's law of heat conduction, the above parameters are related as,

$$Q = kA\frac{(T_1 - T_2)}{\Delta x} = kA\frac{\delta T}{\delta x} \tag{2.1}$$

When $\Delta x \to 0$, this reduces to differential equation form,

$$Q = kA\frac{dT}{dx} \tag{2.2}$$

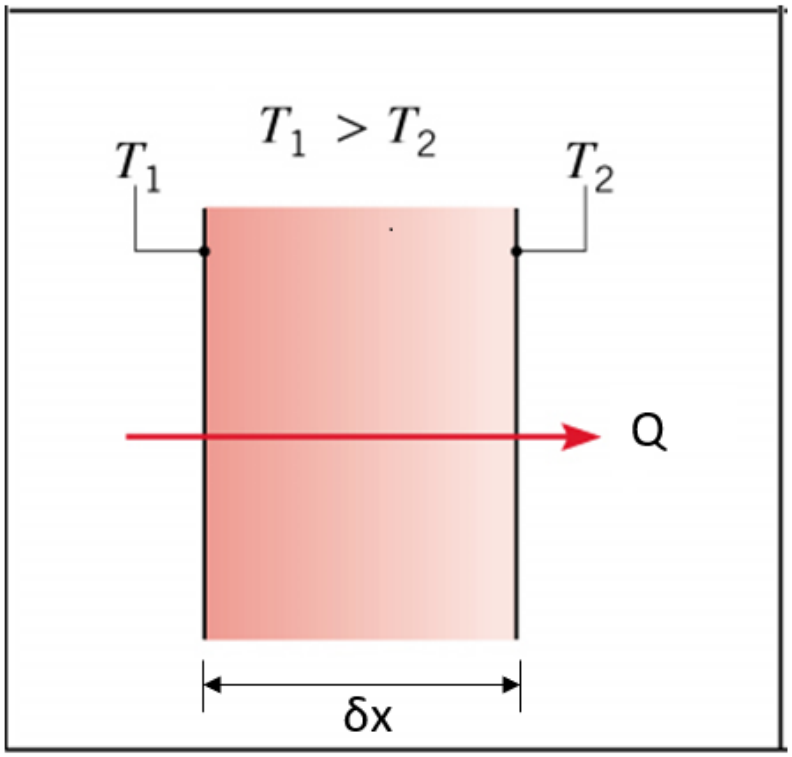

Figure 2.1: Heat transfer through conduction [5]

In Equation 2.2, k [W/mK] stands for thermal conductivity which is the characterisation of the material's ability to conduct heat. Thermal conductivity is also depends on temperature at which it is being operated, hence it varies with change in operating temperatures. Equation 2.2 corresponds to heat flow in x-direction. When the heat transfer takes place through all three primary directions within the body, as shown in Figure 2.2 it is called as 3-dimensional (3-D) heat transfer and is given by equations 2.3 and 2.4.

$$Q_{total} = Q_x + Q_y + Q_z \tag{2.3}$$

$$Q = k_x A_x\frac{dT}{dx} + k_y A_y\frac{dT}{dy} + k_z A_z\frac{dT}{dz} \tag{2.4}$$

For isotropic materials, $k_x = k_y = k_z$ whereas for anisotropic materials, $k_x \neq k_y \neq k_z$.

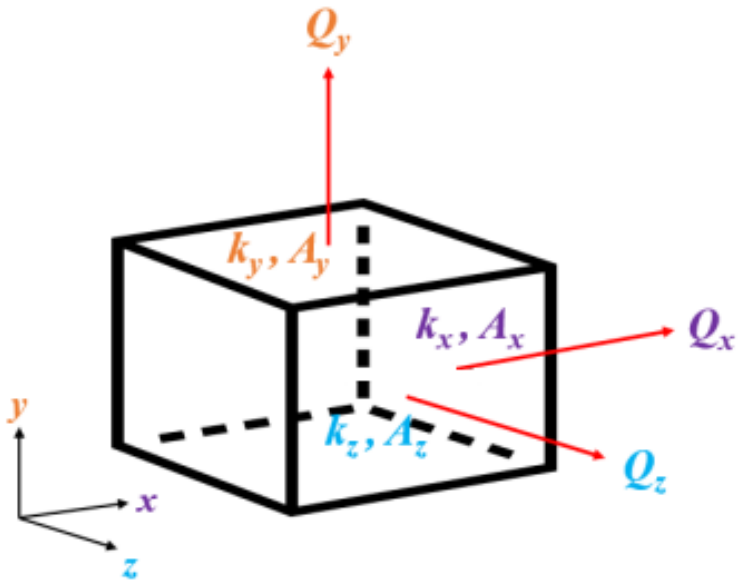

Figure 2.2: 3D heat transfer by conduction [5]

2.1.2 Steady State and Transient Operation

Consider a specific small volume of a one dimensional object, where there is a continuous exchange of thermal energy. A measurable quantity of heat flows into the volume which is Q_{in} and a different quantity of heat flows out of the same volume which is Q_{out}. The difference in these quantities gives the rate of change of energy of the volume which is $\frac{dEvol}{dt}$ [5]. Then these parameters are related as in this Equation 2.5,

$$\frac{dEvol}{dt} = Q_{in} - Q_{out} \tag{2.5}$$

When the rate of energy change tends towards zero the object has attained a state called thermal equilibrium. This is state is achieved when a time-dependent process is executed for a longer period of time, which results in the state where the all dependent parameters attain equilibrium state. When the change in time does not affect the state of the system, the object has attained steady-state. This transforms the Equation 2.5 as the term $\frac{dEvol}{dt}$ becomes zero.

$$Q_{in} = Q_{out} = 0 \tag{2.6}$$

$$Q_{in} = Q_{out} = Q_{conduction} = kA\frac{(T_1 - T_2)}{t} \tag{2.7}$$

In the Equation 2.7, T1 and T2 are wall temperatures at entry and exit of the volume respectively, whereas k and A are thermal conductivity of the object and cross-sectional area perpendicular to the heat flow. t represents thickness of the object parallel to the heat flow. When we compare this Equation 2.7 to the electrical circuit with temperatures is analogical to electrical potential and heat flow to electric

current and the thermal resistance R_{therm} is also be analogus, which is defined in the Equation 2.8

$$R_{therm} = \frac{t}{kA} \tag{2.8}$$

In reality, most of the heat transfer processes are transient in nature as the duration is pretty short to fulfil the application demands and hence a steady-state is rarely attained. Especially in this thesis work, the heat generated by the battery varies continuously with time and a lumped system analysis is a method to solve for the temperature while assuming uniformity throughout the study volume.

2.2 Li-ion Cells

Lithium ion cells consists of an electrolyte and two electrodes as depicted in Figure 2.3 Cathode is the negative electrode, and anode is the positive electrode, where the

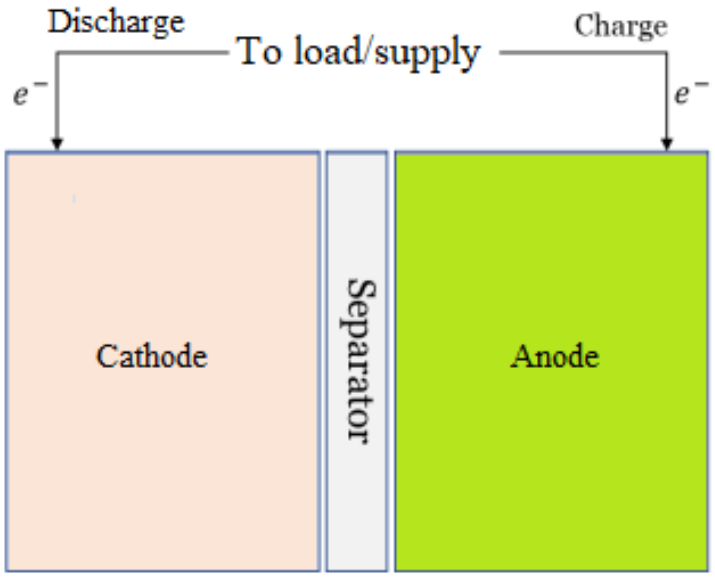

Figure 2.3: Li-ion cell [6]

lithium ions are located when the battery is discharged. The electrolyte also has a separator, which acts as the boundary between the anode and cathode, lithium ions move through the electrolyte from positive to negative electrode during the charge and vice versa while discharging. During charging, the lithium ions carry the electrons in the the positive electrode, and the electrolyte allows only ions to pass through them, when is battery is connected to the external circuit which has the loads, flow reversal happens as the electrons flow from negative to positive, and so the battery is discharging [6].

2.2.1 Lithium Metal Cells

Instead of using typical graphite material as the anode which is the predominant anode material in Li-ion cells, using lithium metal as the anode is being considered as it is improving the energy density of rechargeable battery as illustrated in Figure 2.4. The emerging LBs with lithium metal anode (LMA) are with different cathodes (i) lithiated metal oxide as cathode material, (ii) Li-S batteries with S (Sulphur) composite as cathode material and (iii) lithium-oxygen (Li-O_2) batteries with O_2 as cathode material are being considered [7].

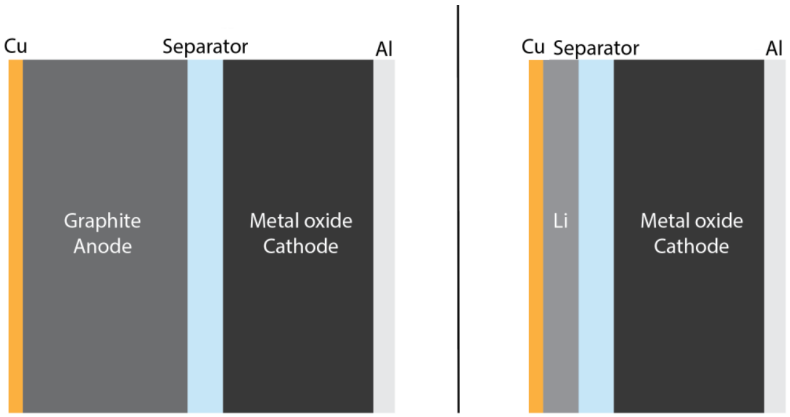

Figure 2.4: Comparison of Li-ion and Li-metal cells

2.2.2 Cell Format

The predominant lithium-ion cell formats at the market are the cylindrical, prismatic, and pouch cells. The various cells have different chemistries, designs, and configurations which are designed in accordance to various applications [8]. The lithium cells can be used both as a primary and secondary batteries. The primary batteries are based on non-electrically reversible chemical reactions which implies that they cannot be recharged and generally used in the electronic devices for a single time usage, whereas the secondary batteries is based on reversible electrochemical reactions, which makes them rechargeable and makes them available for longer period of time and usage. The energy density of LIBs makes them suitable for different applications and different markets such as EV, Portable devices and BES [8].

2.2.3 Pouch Cell

The cell format considered in this thesis work are pouch cells, the characterisation and the construction of pouch cells are explained below.

2.2.3.1 Cell construction

Instead of using a metallic cylinder or a glass-to-metal electrical feed-through like a cylindrical or prismatic cells, pouch cells utilises conductive foil-tabs are welded

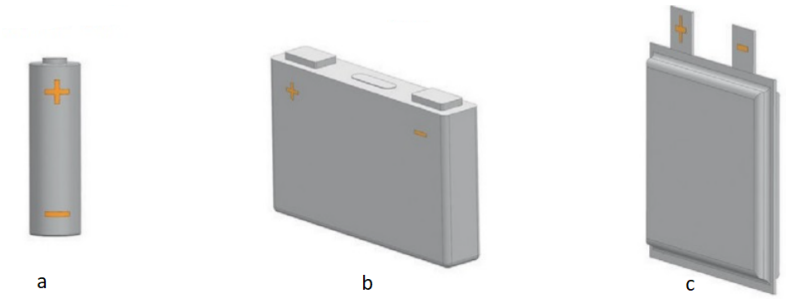

Figure 2.5: Cell Format (a)Cylindrical (b) Prismatic (c) Pouch [9]

to the electrodes and they are fully sealed outside utilising the "pouch" structure outside where the positive and negative terminals are welded respectively . Figure 2.6 illustrates the construction and the layers of the pouch cells.

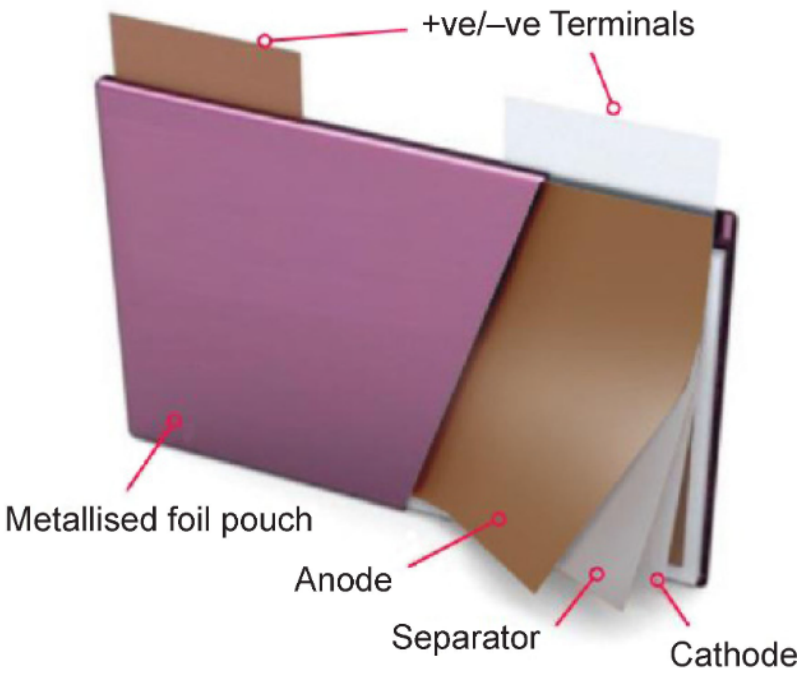

Figure 2.6: Pouch cell construction [10]

They are the most effective battery solution for portable applications which require high current load, such as drones and hobby gadgets. The pouch cells can deliver high load currents but it performs best under light loading conditions and with moderate charging Some stack pressure is recommended but allowance for swelling must also be made. The pouch cells can deliver high load currents but it performs best under light loading conditions and with moderate charging. As the pouch cell offers a simple, flexible and lightweight solution to battery design even with the downside of stack pressure and allowance for swelling as illustrated in the the Figure 2.7 [9].

Figure 2.7: Cell swelling [9]

The pouch cell are the most efficient when the usage of space is considered as it achieves 90–95 percent packaging efficiency. Eliminating the metal enclosure reduces weight, but the cell needs support and allowance to expand in the battery module or in the pack design [9].

2.2.4 Cell Terminologies

There are few general terminologies associated with batteries which are briefly described in this section below.

1. Energy: The power delivered by a cell at instantaneous C-rates for specified times at corresponding battery voltage is called energy delivered by the battery. It is expressed in watt-hours [Wh]. It is obtained by multiplying discharge power with discharge time [11].

2. State of charge (SoC): SoC is defined as the remaining charge capacity within a battery which is expressed as a fraction of current available capacity to its maximum capacity. It is one of the most common terms which one can observe on electronic/-electrical devices expressed in % [11].

3. Depth of discharge (DoD): The amount of charge which has been consumed at a point in time during the discharge cycle is called as depth of discharge. It is opposite to that of SoC and is generally represented in %. When a battery is fully charged, its SoC is 100%, while DoD is 0% and vice-versa is also true, i.e, when its Soc is 0%

and DoD is 100% which signifies that the battery is fully discharged [11].

$$DoD\% = 100 - SoC\% \tag{2.9}$$

4. Capacity: The capacity of the battery is defined as the charge content of a battery which is often in expressed in Ah (ampere-hour) [11]. The battery is considered to be fully charged When the SoC is at 100%,and at lowest when SoC is 0%. For example, a battery of capacity 17 Ah is fully discharged if a constant current of 17 A is drawn for an hour when the battery is fully charged state i.e., from 100% SoC to 0% SoC.

5. C-rate: C-rate is the current rate at which a battery is charged or discharged which is expressed in A (ampere). For example, C-rate of 1C for a 17 Ah cell means a constant current of 17 A, whereas 3C is $17 \times 3 = 51$ A. When a fully charged cell is discharged at 1C and 3C respectively, it theoretically discharges the cell fully in 1 hour and 0.33 hour respectively [11].

5. Internal resistance (R_{int}): The opposition offered to the flow when the circuit is completely open or closed is called as internal resistance. It is a function of temperature and SoC. It is often depicted in the order of mΩ [11].

2.2.5 Heat Generation

Heat generation in lithium-ion batteries occurs both due to reversible and irreversible reactions in the cell. Reversible heat is due to the isentropic heat that originates at the electrodes and arises from reversible entropy change due to the electrochemical reactions. Irreversible heat which is generated at electrodes, electrolytes, and current collectors contributes to 70% of the total produced amount. It is called to as the ohmic heating of a battery cell and is directly dependent on the C-rate varies with cell temperature [12]. From the Figure 2.8 it is clearly evident that as the discharge rate increases heat generation also increases.
The most standardised formula defining heat generation in a battery cell during an electro-chemical reaction is given by the Equation 2.10 [12].

$$Q = I\left(V_o - V\right) - IT\frac{dV_0}{dT} \tag{2.10}$$

In the above equation Q stands for heat generation, I represents the applied current, V_os the open-circuit voltage, and V is the actual cell voltage. The first term $I\left(V_o - V\right)$ accounts for the irreversible losses in the cell. The term on the right defines entropic heat. The cell voltage V deviates from the open-circuit voltage V_os when the current starts flowing in the battery. This happens due to electro-chemical polarization and the resulting energy loss transforms into heat [12].

$$Q_{irr} = I\left(V_o - V\right) = I^2 R_{int} \tag{2.11}$$

Here in this equation 2.11 Q_irr represents heat generated during charge/discharge cycle, while R_{int} stands for over-potential resistance

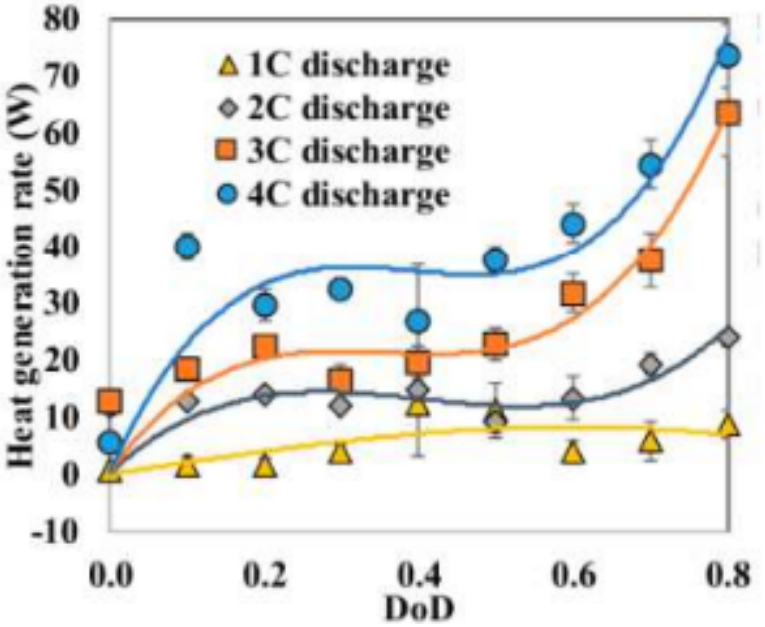

Figure 2.8: Heat generation Vs DoD [12]

Ohmic heating is due to the the internal resistance of a battery, and this resistance is a function of the state of charge and temperature as depicted in the Figure 2.9. Higher internal resistance can be observed under lower battery operating temperatures. Moreover, this ohmic resistance is lowest at the SOC of 60-90% and higest with lower and higher SOC [13].

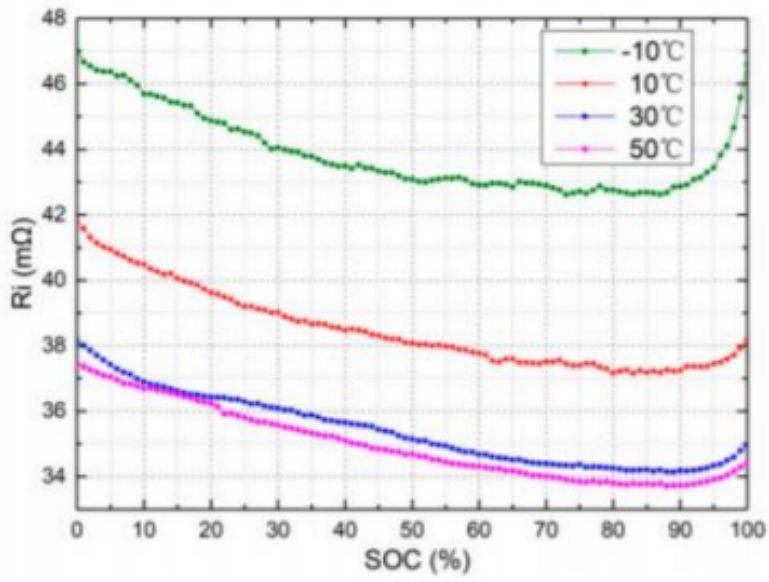

Figure 2.9: Dependence of internal resistance on the operating temperature and SOC [13]

2.2.6 Thermal Management

Performance of lithium-ion cell dependents directly on the cell operating temperature. Hence, it is necessary to main the temperature of the cell within its operating range. Lithium batteries have an optimum working temperature at 15-35°C [3]. When it is operated outside this range, it will have a long lasting impact on the performance and lifetime of the batteries. The most important factors are discussed below

2.2.6.1 Capacity fade:

When exceeding an optimal temperature of a cell will lead to increase in the cell internal resistances which in turn will reduce the performance and the capacity of the cells. In addition this, higher operating temperatures will increase the cycle performance loss and also loss is the capacity of the cells when it is cycled. Cells that operate at higher temperature have a higher capacity loss after each cycle in comparison will cell at lower temperatures this is due to the phenomenon called lithium plating which results in loss of lithium-ions and a shorter lifespan [14].

2.2.6.2 Thermal Runaway:

As the cell temperature increases above the operating limit, it will cause a series of undesirable exothermic reactions to occur which will further increase the temperature. If this happens, it creates a continuous chain type reaction and results in the event called thermal runaway. An experimental study was conducted on Li-ion batteries showed that the highest temperature which was recorded was found to be 870 °C internal cell temperature. This lead to a thermal runaway event. If the event is not controlled this could cause severe fire and explosion. The different reasons that thermal runaway could occur is due to high temperature, overcharge, short circuiting and nail penetration [15].

2.2.7 Cooling Strategies

As explained in the previous sections, inappropriate battery temperature will have a severe effects on many different aspects. Hence, BTMS is required for every battery system. The primary duty of a BTMS is to keep the batteries in the optimum temperature range and maintain an even temperature distribution. The most common thermal management methods for battery packs are reviewed here.

2.2.7.1 Direct Cooling:

When the heat is removed directly with cooling medium it is called as direct cooling, Direct cooling, also known as immersion cooling, covers the entire surface of the cell and cools it uniformly. The main advantage of this strategy is to overcome hot/cold spots in the cell and thereby increasing the performance. The biggest challenge is to developing the coolant for direct cooling as the ideal coolant should be dielectric with low viscosity and high thermal conductivity and thermal capacity [16]. Figure 2.10 shows the example of immersion cooling technology. Owing to its cost and

complexity, immersion cooling is predominantly used in data center servers and power electronics. .

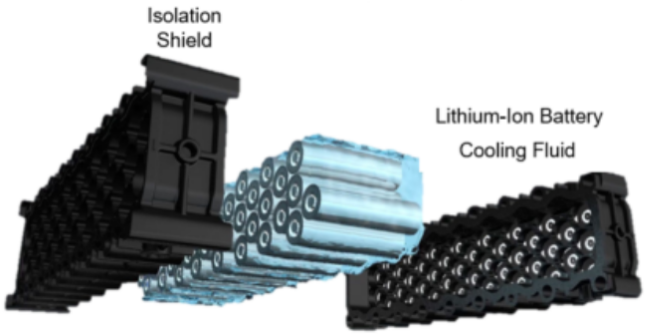

Figure 2.10: Immersion cooling [16]

2.2.7.2 Indirect Cooling:

Indirect liquid cooling is a strategy which is achieve by enabled the conducting heat to the ambience through a medium or a heat exchanger. This type of thermal management is adopted by different industries and commonly used in electric vehicles owing to its heat transfer, safety and reliability. The liquid cooling system has been widely developed and adopted in recent years due to its cooling performance over air cooling.When the heat dissipation is accomplished only by ambient cooling it is passive cooling,and when the cooling or heat is accompoloshied by external source it is called as active cooling. The most commonly adapted active cooling is through heat exchangers which utilises indirect cooling by corrugated cooling channel and a cold plate. The Figure 2.11 is a well known example for corrugated cooling channel which is also called as serpentine cooling pipe, from Tesla Model S [17],

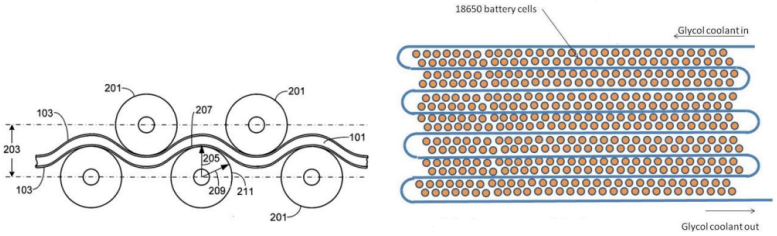

Figure 2.11: Corrugated channel from Tesla S [17]

2.2.8 Heating

Thermal management includes both cooling and heating strategies of the batteries. However, only certain studies have been done to determine different ways of heating. This could be due to the exothermic nature of battery operation as there will always

be natural heating from the operation of the cells. As, low operating temperature will only degrade the performance and life out of the batteries. Heating up the cells is analogous to the cooling strategy and also the time it takes to heat the batteries to the optimum temperature range. Heating of lithium cells from sub-zero up to ideal temperatures could be accomplished into three different strategies, namely convective heating, self-internal heating, and mutual pulse heating [4].

2.2.8.1 Self-internal heating:

At low temperatures, the internal resistance of the cells is higher, therefore more heat will be generated inside the cells as they start to operate. As the cells started to operated even while charging and discharging the temperature steadily reaches the optimum temperature range and then it facilities higher charge and discharge profiles. The main downside is degrading calendar life even though the cells are operated at very less charge and discharge profile [4].

2.2.8.2 Convective heating:

The batteries themselves supply a small potential to the electric heater and a fan. The air is which is forced down by the fan over the electric heater, heats the cells up by convective heat transfer [4].

2.2.8.3 Mutual pulse heating:

The batteries are divided into two or more groups. One group is discharged to charge the other group of batteries and the other group is discharged to charge the previous group. This cycle is alternatively repeated between the groups. This method is quite faster when compared to the internal heating and it provides more reliable and uniform heating compared to convective heating. This method uses least battery capacity than the other methods described. The biggest downside of this method is the cost due to a more complex temperature sensing and control systems to switch the charge and discharge profiles [4].

3
Methodology

In this chapter, the entire workflow of the thesis work is elaborated and also the different cases and their setup in Star-CCM+ are explained. The project was split into two studies, where the first study comprises of a simple model involving a cell is used to verify different cooling strategies available on the cell level. Then the feasible solutions were selected for the next set of iterations which included other components. Finally, these results are validated by experimental results

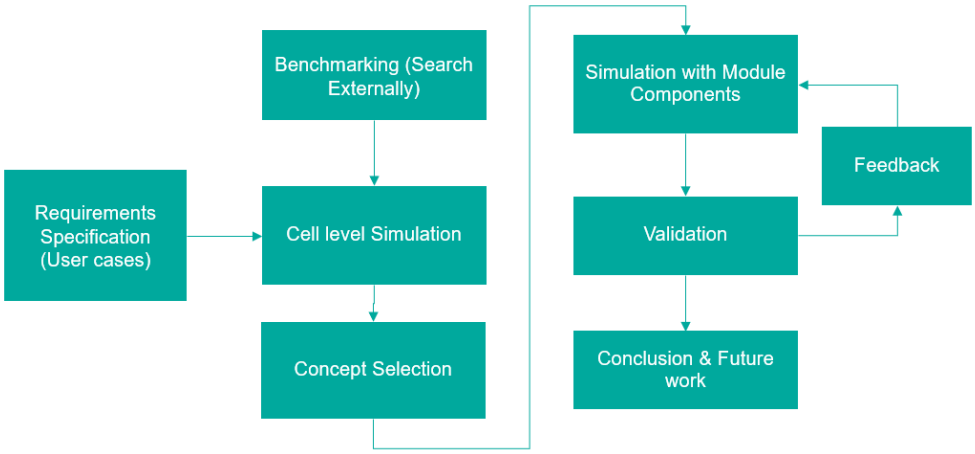

Figure 3.1: Thesis workflow

The structured workflow as listed in the Figure. 3.1 is utilised to solve the problem, as it eliminates uncertainties and non feasible solutions and will lead to feasible solutions [18].

3.1 Benchmarking

The literature study and benchmarking was carried out based on the research questions framed for the thesis work. Initially, the study was carried out with a wider scope of search on the different strategies and methodologies of cooling the battery module using commercial benchmarking tool a2mac [19]. Later the study was gradually narrowed to the cell level as it is the smallest building block on which different level such as modules and packs are built upon. The initial search utilised both the

methods searching internally and searching externally as defined in product development terms [18]. Initially, the different competitor battery modules products were identified and selection of modules were based on cell format. The benchmarking gave insights to different type of thermal interface, cooling characteristics, charge and discharge profiles. Based on insights from the benchmarking ideas and key parameters which are necessary for further development of cooling concepts were identified. The results of the benchmarking are in the Appendix A

3.2 Test cases

- 3C discharge from 0% DOD to 100%. Maximum temperature limit +60°C.
- Heat up of cell from -55°C to +25°C within 60 min with a temperature uniformity of ±5 degree (based on Aviation Standard DO-160)

3.3 Simulation Setup in Star CCM+

This sections deals with the different sets of simulations that were performed using commercial CFD software star CCM+. The sections listed will briefly discuss about the meshing parameters, assumptions and boundary conditions employed in star CCM+

3.3.1 Cell Level Simulations

Creating the 3-D thermal model of a Li-ion pouch cell is one of the objectives of this thesis work. All of the geometric and material parameters of the individual material properties of anode, separator, cathode and electrolyte are industry secrets and due to confidentiality. Hence, a lumped material with equivalent material properties was used in the simulation model [20]. Density, specific heat capacity and thermal conductivity were calibrated according to the experimentally calculated values. Figure 3.2 shows the reference axes used for the cell geometry along with in and through-plane directions.

3.3.1.1 Meshing

As shown in Figure 3.3, 3.4 polyhedral mesh was created as it provides good accuracy with lower memory and computational power demand and also these could also be integrated with the necessary fluid domain. Approximately 100,000 Cells were generated with the help of star CCM+. As, discussed earlier Cell is modelled as a single lumped object. The physical properties were created by utilising the material properties which are density (Kg/m3), specific Heat Capacity (J/Kg-K) and thermal Conductivity (W/m-K).

3.3.1.2 Boundary Conditions

As, these simulations are used to find out the feasible concepts the most idealistic considerations were made. An initial temperature of 25°C was considered for the

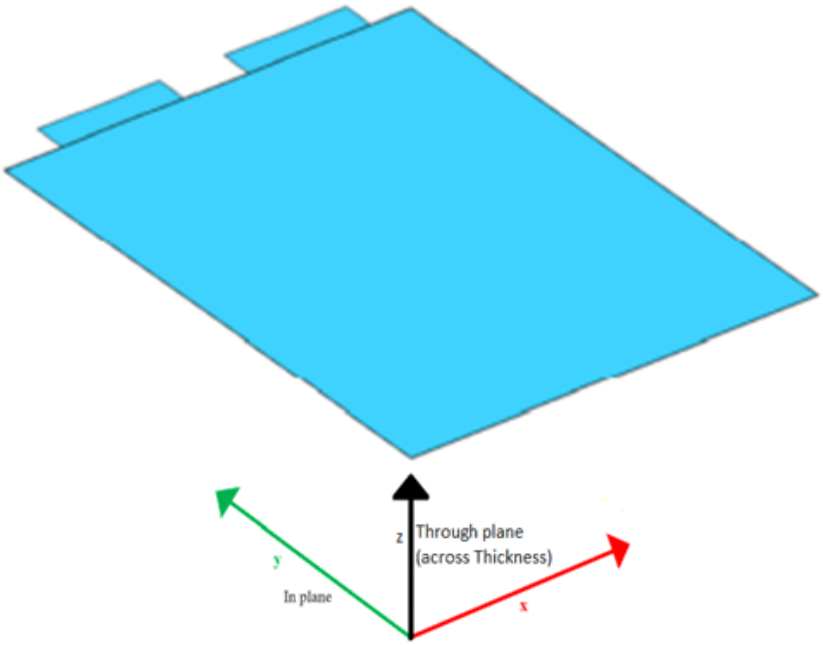

Figure 3.2: Geometry of the cell illustrating in plane and through plane axes

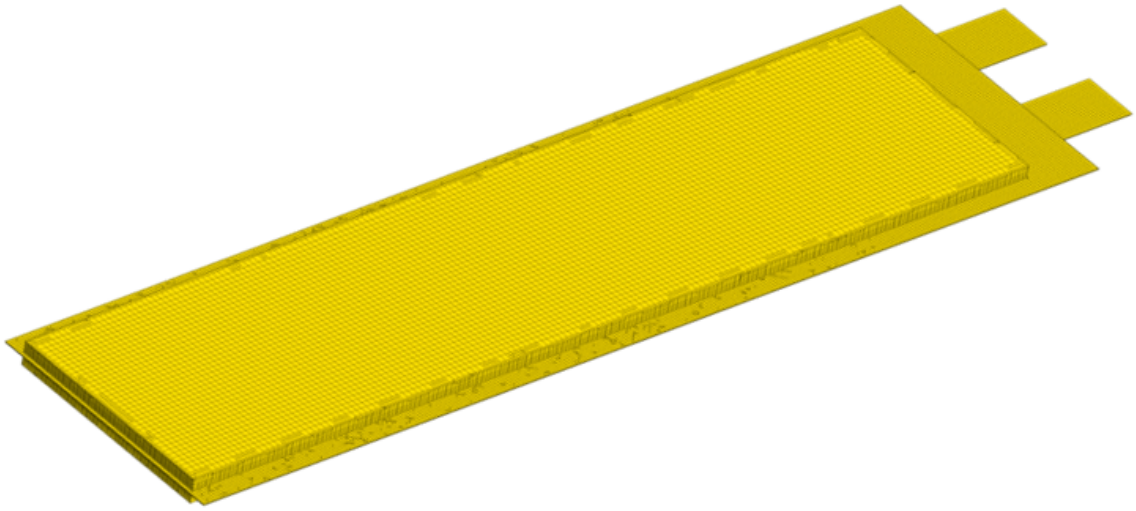

Figure 3.3: Iso view of meshed cell

entire unit cell. This was based on the assumption that the cell was not operated for a significant amount of time and stored at room temperature where the ambient temperature is controlled. The faces which were exposed to cooling interface was assumed to be at 20°C and it was also assumed that the cooling system will be able to deliver constant cooling depending on the heat generated. Apart from these faces, rest all faces are assumed to be adiabatic.

Figure 3.4: Section view of meshed cell

3.3.2 Module Simulations

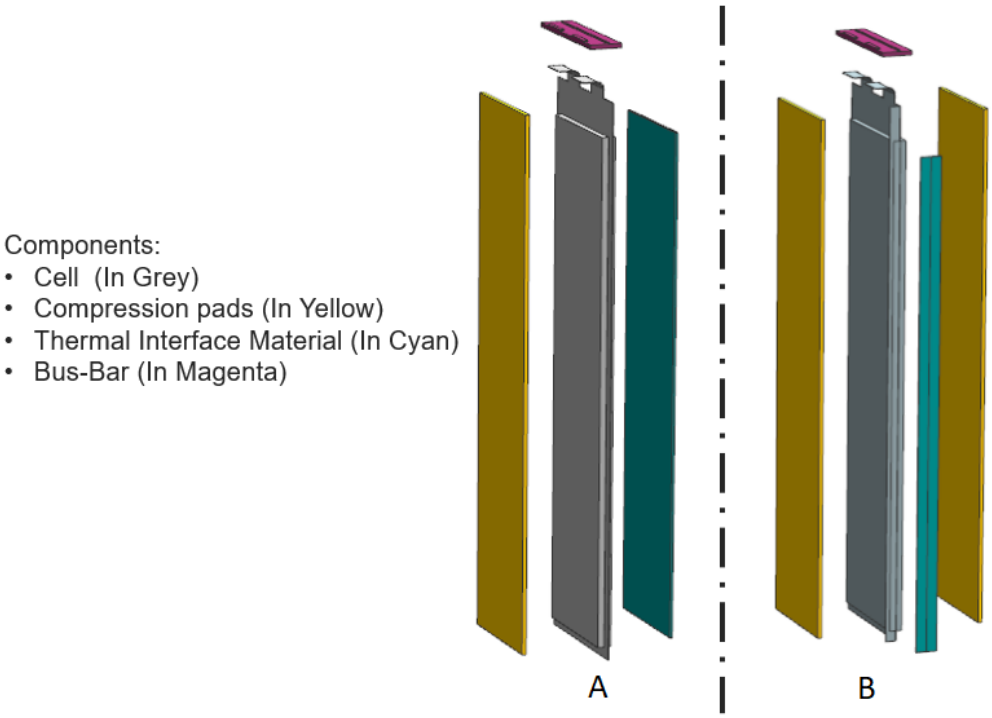

Figure 3.5: Module concepts with (A) Radial cooling ,(B) Long sided cooling

The results from the previous sets of simulation allowed for the selection of concepts which were further developed in the simulation environment by including the module components. Figure 3.5 illustrates the different components used in this set of simulations.

3.3.2.1 Meshing

As shown in Figure 3.6, polyhedral mesh was generated with approximately 900,000 Cells. Generated mesh was conformal to have proper interactions with surrounding objects which is depicted in the Figure3.7. Cell is modelled as a single lumped object. Four different physical regions were created in star CCM+ to map the correct material properties of the different materials. The material properties utilised

are density (Kg/m^3), specific Heat Capacity (J/KgK) and thermal Conductivity (W/mK).

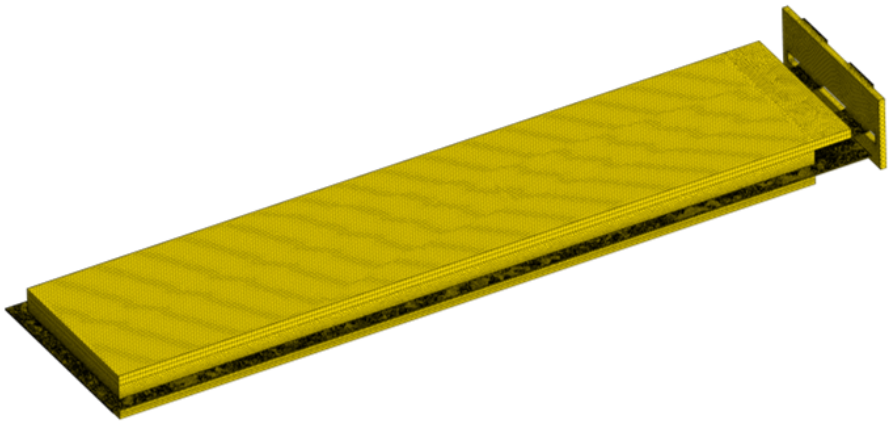

Figure 3.6: ISO view of meshed module

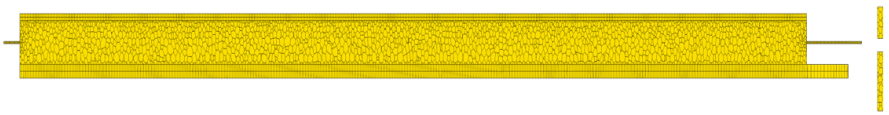

Figure 3.7: Section view of meshed module

3.3.2.2 Boundary Conditions

As, these simulations are used to find out the feasible concepts the most idealistic considerations were made. An initial temperature of 25°C was considered for the entire unit cell. This was based on the assumption that the cell was not operated for a significant amount of time and stored at room temperature where the ambient temperature is controlled. The faces which were exposed to cooling interface was assumed to be at 20°C and it was also assumed that the cooling system will be able to deliver constant cooling depending on the heat generated. Apart from these faces, rest all faces are assumed to be adiabatic.

3.4 Test Setup

A hybrid test was constructed for this work. Figure 3.8 shows the schematic layout of the constructed test setup. Commercially available electronic load box and power supply was used to charge the discharge the cells. The electrical connections were made in such a way that the charging and discharging connections were separate for safety reasons. It also allowed to use the existing power capacities of the lab to

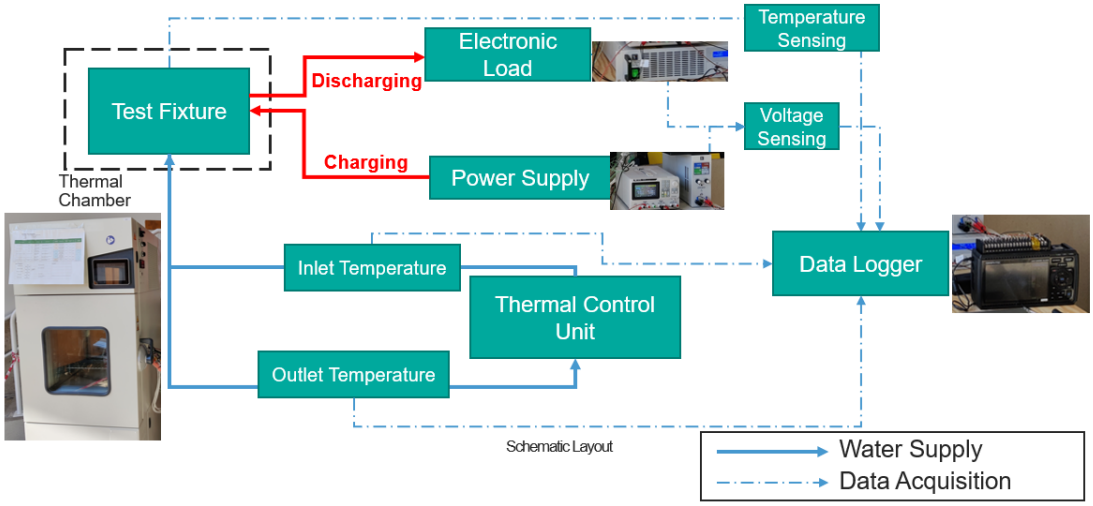

Figure 3.8: Schematic layout of test setup

charge and discharge the cell in safe manner. As the test cases involve both heating and cooling criterion, thermal chamber was used to maintain the necessary ambient conditions. The voltage, current and temperature of the cell were also monitored by a Data logger as depicted in the Figure 3.8. The inlet and outlet temperature of the water entering the cold-plate was also monitored. The data logger logs the necessary values at one second intervals which was then post-process using Excel and Matlab.

3.4.1 Compression Rig

A special isolating rig was created for tests that include active cooling using the battery cooling. The rig was created to isolate the cell from the ambient thermal environment and maintain compression of the cooling plate to battery surface interface. In order to have a much uniform contact TIM (Thermal Interface Material) was used between the cooling plate and the battery surface. An exploded CAD view of assembly is shown in Figures 3.9 & 3.10

Figure 3.9 represents the test fixture for the radial cooling and Figure 3.10 represents the test fixture for the long sided cooling.The rig is comprised of two 15.0 mm thick polycarbonate sheets with the battery and cooling plates sandwiched between the two sheets. Holes are present in each corner to allow a threaded bolt to pass through. By tightening down the bolt fasteners, the battery is confined to the assembly predefined assembly pressure necessary to charge and discharge the cells. Spacers were constructed using polycarbonate sheets with thickness was based on the calculated thickness values to keep the necessary compressive force.

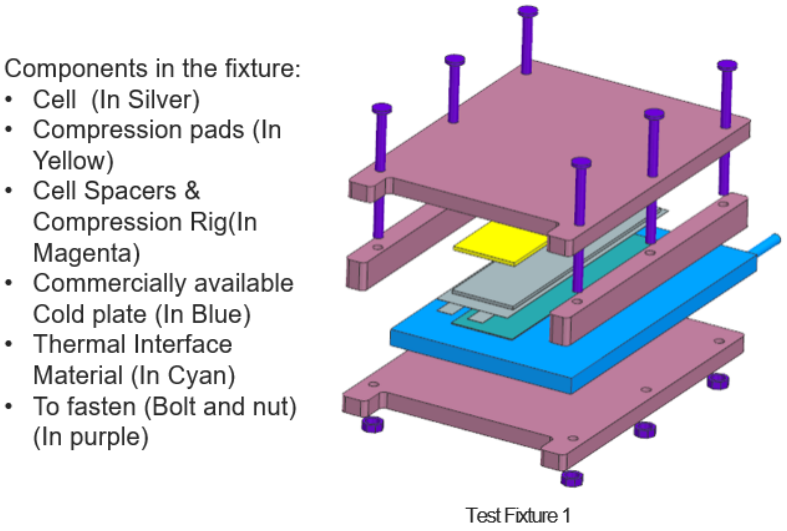

Figure 3.9: Exploded view of test fixture 1

3.4.2 Calculation Methodology

Thermistors were installed on the principal surfaces of the battery to measure temperatures at 14 discrete points, which corresponds to 28 points in total. These thermistors utilizes a multi-junction construction on a polyaimide film laminate which are then adhered to the battery surface using Kapton backed adhesive tape as shown in Figure 3.11. Two additional K-type thermocouples were used on one side of the compression pad to determine the heat absorbed by the compression pads which is again adhered using Kapton tapes 3.12.
Equation 3.1 is used to evaluate the sensible heat energy stored in the battery when the battery temperature changes from an initial temperature to a final temperature.

$$Q_{Total} = Q_{Stored} + Q_{Removed} + Q_{Environment} \tag{3.1}$$

A method was devised to determine the average temperature across the entire battery surface. For each thermistors, it is assumed that the measured temperature represents the average of an area extending around the sensor. The areas are determined by defining each area boundary by calculating the x and y midpoint distance between adjacent sensors.

$$Q_{Stored} = Q_{Sensible} = m_{battery} C_{p,battery} (T_{t2} - T_{t1}) \tag{3.2}$$

Equation 3.1 is used to evaluate the average battery surface temperature by summing the temperature-area products and dividing by the total area of the surface.
The rate of sensible heat accumulation is directly influenced by the battery heat generation rate. The temperature of the battery increases as heat is generated due to the finite heat transfer to the surrounding. The rate of sensible heat accumulation is determined from the rate of change of Equation 3.3.

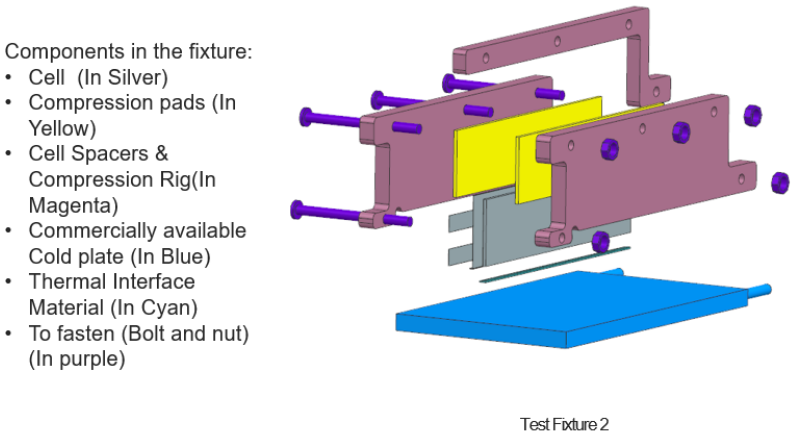

Figure 3.10: Exploded view of test fixture 2

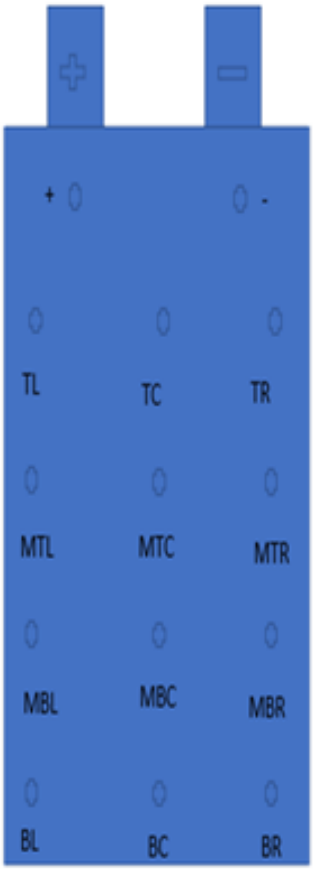

Figure 3.11: Temperature measurement points on the cell

$$Q_{Stored} = m_{battery} C_{p,battery} (\frac{dT}{dt}) \tag{3.3}$$

where $\frac{dT}{dt}$is the rate of temperature change in the battery and rate of temperature

Figure 3.12: Temperature measurement points on the compression pad

change is calculated by measuring the temperature over a time interval and calculated using Equation 3.4.

$$\frac{dT}{dt} = \frac{T_{t2} - T_{t1}}{t_2 - t_1} \tag{3.4}$$

Using the above Equations 3.3 & 3.4, Equation 3.2 is transformed as

$$Q_{Stored} = m_{battery} C_{p,battery} (\frac{T_{t2} - T_{t1}}{t_2 - t_1}) \tag{3.5}$$

Heat removed from the Cooling plate is determined by the inlet and outlet temperature data recorded, in conjunction with the recorded flow rates. The difference in inlet and outlet temperatures is the heat conducted from the battery surface. The heat removed by a cooling plate is calculated using Equation 3.6

$$Q_{Removed} = Q_{coolingplate} = m_{water} C_{p,water} (T_{Outlet} - T_{Inlet}) \tag{3.6}$$

The total amount of heat removed by the cooling plates for a time period Δt can be determined using Equation 3.7

$$Q_{coolingplate} = m_{water} C_{p,water} (T_{Outlet,avg} - T_{Inlet,avg}) \Delta t \tag{3.7}$$

The terms $T_{Outlet,avg}$&$T_{Inlet,avg}$ in Equation 3.7 is the average of measured outlet temperature and inlet temperatures during the period Δt, as in Equation 3.8 which is also true for inlet conditions. N represents the number of temperature readings in the summation.

$$T_{Outlet,avg} = \frac{\Sigma T_{Outlet}}{N} \tag{3.8}$$

$$Q_{Environment} = Q_{Compression-pad} = kA\frac{dT}{dx} \tag{3.9}$$

The Equation 3.9 is used to estimate the heat absorbed by the compression pad. As the tests are performed with the ambient conditions i.e, the temperature maintained in the thermal chamber and the temperature of the water maintained the same. Ideally there is no heat transfer between the cooling plate and the ambient conditions, To ensure there is no heat losses, inlet and outlet temperatures were monitored before the start of the tests and if there is difference in the temperature this additional heat is measured as temperature difference between the inlets and outlets.In order to evaluate this effect, the cooling system and thermal data acquisition was activated with the battery in place but no charging or discharging occurring. In this way, the temperature difference between the inlet and outlet of each cooling plate could be recorded.

4

Results

In this chapter, the results are presented in the chronological order of the work flow: the solution for the cell simulations are presented first which includes comparison of different cooling concepts on the cell level followed by the comparative study on the transient and steady state simulations. In the second part, the results of the module simulations is discussed which is then compared to the experimental results. Certain values from the simulation and also from the experiments could not be shared due to confidentiality reasons.

4.1 Cell Simulations

As discussed in Section 3.3.1 for cooling strategies were simulated on the cell level. The concepts are listed are compared in the subsequent sections.

4.1.1 Steady state

This section briefly discusses about the results of steady state simulations which is based on the assumption that the heat generated within the cell is steady throughout the time period. Four different cooling strategies which were developed are compared against each other.

Table 4.1: Radial cooling Vs Long sided

Concept	Temperature Contour	Thermal Resistance (K/W) StarCCM+ (R= ΔT/Q)	Thermal Resistance (K/W) Geometrical (R= t/(k*A))
Radial Cooling 	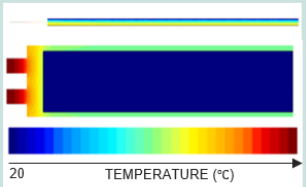	0.356	0.345
Long Side 	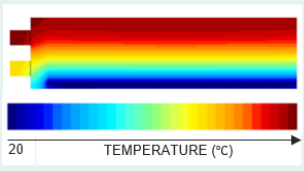	0.757	0.818

Table 4.1 compares radial cooling with long side cooling. Results from the simulation showed that the radial cooling has a thermal resistance 0.356 (K/W) while long sided cooling has 0.757 (K/W). This Resistance was calculated by calculating the temperature difference (ΔT) of maximum temperature (T_{max}), minimum temperature (T_{min}) upon the Heat conducted (Q). From the temperature contours it is also evident that the maximum heat is accumulated at the terminals in the case of radial cooling. On the other hand, the maximum temperature is distributed at the extreme end of the cell opposite to the cooling terminal in the case of long sided cooling. These thermal resistance values are compared against the thermal resistance values which was calculated using Equation 2.8 based on the geometrical parameters as discussed in the section 2.1.2.

Table 4.2: Terminal cooling Vs Short side

Concept	Temperature Contour	Thermal Resistance (K/W) StarCCM+ (R= ΔT/Q)	Thermal Resistance (K/W) Geometrical (R= t/(k*A))
Terminal Cooling 	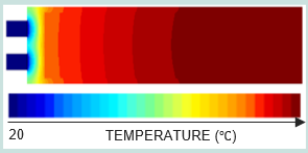	19.8	20.1
Tab + Short Side cooling 	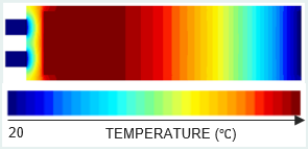	5.6	5.03

Table 4.2 compares terminal cooling & terminal cooling with short side cooling. Results from the simulation showed that the radial cooling has a thermal resistance 19.8 (K/W) while terminal cooling + short-side has 5.6 (K/W), from these results it is clear that these two cooling strategies are ineffective due to the geometric nature of the cell which is envisioned by the thermal resistance. From the illustrated temperature contours it is clear that the heat is accumulated at the bottom of the cell in the case of terminal cooling. On the other hand, the maximum temperature is distributed at the top end of the cell closer to the terminals when both the short sides are cooled.

4.1.2 Steady state Vs Transient

As, discussed in the section 2.2.5 heat generation is transient and it is entirely depending on the charge and discharge rates. This set of simulations were performed with the transient heat generation data which is then compared with the steady state results.
Table 4.3 compares radial cooling and long sided cooing with the thermal resistance values of both steady state and transient simulations. Thermal resistance results

Table 4.3: Transient Vs Steady

Concept	Thermal Resistance (K/W) Transient	Thermal Resistance (K/W) Steady	% change in T_{max} between Transient and Steady state
Radial Cooling 	0.3	0.303	1.5% increase (Transient > Steady-state)
Long Side 	0.753	0.757	2.2% increase (Transient > Steady-state)

from the simulation showed that the steady state and transient values were almost the same, as the heat generation increases, the maximum temperature (T_{max}) also increases. Hence, the resistance value was constant over the whole operating time. Hence, it was necessary to compare the % increase of (T_{max}) from transient to steady. The increase in (T_{max}) was approximately around 2% which is due to sudden increase in the heat generation towards the end of discharge in the case of transient simulation.

4.1.3 Remarks

From, these sets of simulations non feasible concepts were identified which are terminal cooling & terminal cooling with side side cooling for the predefined conditions. Hence, they are excluded from the further development. As the steady state simulations gave comparable results with transient simulations, next set of iterations could be performed in steady-state conditions rather than in transient conditions. Cooling the short side alone is non-effective owing to the geometric nature of the cell.

4.2 Module Simulations

As discussed in the Section 3.3.2, concepts which were selected are added into the module environment and further validated within the steady state condition. The results are tabulated in the Table 4.4 below. From the results it is clear that the cooling strategies follow the similar trends as the previous set of steady state simulations. The slight increase to the thermal resistance is to the added components

Table 4.4: Module Simulation

Cooling Concept	Simulated Results	Thermal Resistance (K/W) StarCCM+ (R= ΔT/Q)	Thermal Resistance (K/W) Geometrical (R= t/(k*A))
Radial Cooling	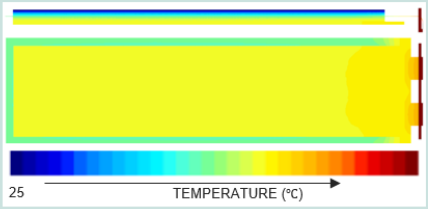	0.372	0.345
Long Side	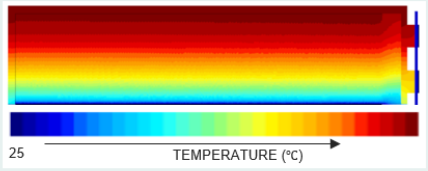	0.758	0.818

which further restricts the the heat flow. The heat concentration happens at the terminals and the bus-bar in the case of radial cooling. while the heat accumulated at the extreme end of the cell opposite to the cooling terminal in the case of long sided cooling.

4.2.1 Simulation Vs Experimental

Table 4.5: Simulation Vs Experimental

Concept	Thermal Resistance (K/W) Geometrical	Thermal Resistance (K/W) Steady	Difference in T_{max} ℃	Heat Generation during cooling
Lateral Cooling/ Radial Cooling Maximum heat generation @76% DOD 	0.34	0.343	Approx. 6.3% (Experimental >Simulated)	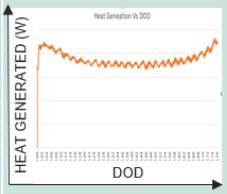
Long Side Cooling Maximum heat generation @77% DOD 	1.21	1.18	Approx. 4.2% (Experimental >Simulated)	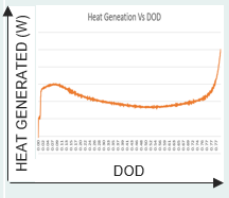

The comparison between Experimental and calculated data is tabulated in the Table 4.5. The change in the Thermal resistance values from the previously calculated values 4.1 is due to the calculated approach previously followed. As, the maximum

and minimum temperature values used here 4.5 is to calculate was accordingly measured in star CCM+ to have a proper correlation between the experimental and simulated results. Heat generation curves were also generated based on calculation methodology described in the section 3.4.2. From, the results it is also evident that the maximum heat generation happens at the end of discharge which is due to the maximum internal resistance at lower SoC.

4.2.2 Heating

Due to the non availability of necessary material properties at sub-zero temperatures, the heating curve couldn't be simulated in star CCM+. Hence, experimental results are of a greater importance. From the thermal resistance values (See Table 4.6), it is evident that the both the experimental results validates themselves. The time taken to reach the temperature homogeneity was also estimated based on the heating curve which was numerically calculated based on the test data. From the results it is also clear that the Radial heating is the most effective way to heat cells and allow them to maintain temperature homogeneity as well. In order to compare the strategies the experiments are conducted in the same conditions. Hence, the heating capacity was not enough for the long sided heating to reach the temperature homogeneity within 60 min. The initial spike in the heating curve is due to sudden increase in surface temperature of the cells which attained steady state as the time progressed.

Table 4.6: Experimental Heating

Concept	Thermal Resistance (K/W) Geometrical	Minimum Temperature 25℃ after	Temperature Homogeneity (T_{max}-T_{min}) ℃	Heating Curve
Lateral Heating/ Radial Heating 	0.34	32 min	5.01	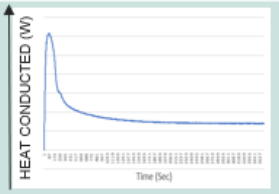
Long Side Heating 	1.21	>60 min	5.45	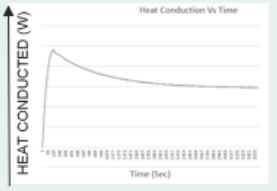

5
Conclusion

The thesis presents the results of CFD studies and experimental studies by investigating a simple cell model and then a simple module concept. Analysis on results of cell level was performed by comparing different cooling concepts based on its thermal resistance characterisation. After studying the effect of both steady state and transient heat generations on the cell, conclusions were drawn to proceed with steady state simulations for subsequent module iterations. The main outcomes from the work are presented below

- From simulations:
  - Both steady state and transient simulations produced very similar results on the cell level.
  - The most effective way to heat and cool the cell is Radial cooling as the area available is significantly larger, even-though the through-plane conductivity is very small on comparing with in-plane conductivity.
  - The long-sided cooling and heating needs higher cooling and heating capacity than the radial in order to achieve temperature homogeneity
- From experiment:
  - Thermal resistance of radial cooling was less than the long sided cooling
  - The trend of thermal resistance of radial heating was less than the long sided heating which is analogous the cooling strategy
  - The heat removed during cooling and heat into the cell is also calculated through which the heat flux is also estimated.
  - The increase is cell surface temperature was towards to end of the discharge at around 76% DoD, which is due to increase in internal resistance of the at highter DoD as discussed in section 2.2.5

5.1 Future Work

A few suggestions for continued work which are based on further iterating and improving the simulation and the test setup are listed below:

- In simulations:
  - Electro-Thermal model to predict the hot-spots as the developed thermal model is not suitable and needs further improvements.
  - A one-Dimensional Thermal model could be developed to validate dynamic load profiles, as they are more suitable for evaluating dynamic profiles rather than the constant discharge profiles which was the scope of this thesis work.

  - Instead of using temperature boundary condition, heat flux boundary condition should be used based on the heat that could be extracted out from the cell. This will have more comparable results to the reality.
  - The developed thermal model could be coupled with cooling system design to further predict the performance of the cooling system.
  - By using Experimental and Simulated results mechanical interface can now be designed and further optimized for different operating conditions.
  - Other factors such as space, cost and manufacturing feasibilities could influence the final concept selection on the module level.
- In Test setup:
  - Insulating the whole fixture so ideally there is no heat losses towards the environment.
  - Time constant to estimate the actual heat loss to the environment.
  - Different test cases than to the one performed to further validate the different operating conditions.

Bibliography

[1] Rebling. The critical role of batteries in the aviation industry. [Online]. Available: https://rebling.com/blog/the-critical-role-of-batteries-in-the-aviation-industry/ (Accessed 2022-02-03).

[2] Markets and Markets. Electric aircraft market. [Online]. Available: https://www.marketsandmarkets.com/Market-Reports/electric-aircraft-market-52646445.html (Accessed 2022-02-03).

[3] W. H. H. Liu, Z. Wei and J. Zhaoa, "Thermal issues about Li-ion batteries and recent progress in battery thermal management systems: A review," *Energy Conversion and Management*, vol. 150, pp. 304–330, 2017, (Accessed 2022-02-03).

[4] Y. Ji and C. Y. Wang, "Heating strategies for Li-ion batteries operated from subzero temperatures," *Electrochimica Acta*, vol. 107, pp. 664–674, 2013, (Accessed 2022-02-03).

[5] A. G. Y. Cengel, *Heat and Mass Transfer - Fundamentals and Applications*. MC GRAW HILL, 2019.

[6] U. of Washington. What is a lithium-ion battery and how does it work? [Online]. Available: https://www.cei.washington.edu/education/science-of-solar/battery-technology/ (Accessed 2022-02-03).

[7] W. O. Library. Lithium metal cells. [Online]. Available: https://onlinelibrary.wiley.com/doi/full/10.1002/advs.202101051 (Accessed 2022-02-03).

[8] B. University. Types of battery cells. [Online]. Available: https://batteryuniversity.com/article/bu-301a-types-of-battery-cells (Accessed 2022-02-03).

[9] M. Technologies. Cylindrical cell vs prismatic cell vs pouch cell. [Online]. Available: https://www.maxworldpower.com/cylindrical-cell-vs-prismatic-cell-vs-pouch-cell/ (Accessed 2022-02-03).

[10] P. Miller, "Automotive Lithium-Ion Batteries: State of the art and future developments in lithium-ion battery packs for passenger car applications," *Johnson Matthey Technol. Rev*, vol. 59, 2015, (Accessed 2022-02-03).

[11] N. Institue. Cylindrical cell vs prismatic cell vs pouch cell. [Online]. Available: https://nickelinstitute.org/en/about-nickel-and-its-applications/nickel-in-batteries/a-guide-to-understanding-battery-specifications/ (Accessed 2022-02-03).

[12] J. K. Yasir Abdul Quadir, T. Laurila and K. Jalkanen, "Heat Generation in High Power Prismatic Li-ion Battery Cell with LiMnNiCoO2 Cathode Mate-

rial," *International Journal of Energy Research*, vol. 38, 2014, (Accessed 2022-02-03).

[13] Y. B. Dian Wang and J. Shi, "Lithium-Ion Battery Internal Resistance Measurement Application in State-of-Charge Estimation," *Energies*, vol. 30, 2017, (Accessed 2022-02-03).

[14] M. W. Sophia Gantenbein, Michael Schönleber and E. Ivers-Tiffée, "Capacity Fade in Lithium-Ion Batteries and Cyclic Aging over Various State-of-Charge Ranges," *Sustainability*, vol. 11, 2019, (Accessed 2022-03-05).

[15] M. O. Xuning Feng and X. He, "Thermal runaway mechanism of lithium ion battery for electric vehicles: A review," *Energy Storage Materials*, vol. 10, pp. 246–267, 2018, (Accessed 2022-03-05).

[16] F. Bridge. Immersion cooling – potential alternative to traditional battery cooling. [Online]. Available: https://www.futurebridge.com/industry/perspectives-mobility/immersion-cooling-potential-alternative-to-traditional-battery-cooling/ (Accessed 2022-02-03).

[17] A. S. Zhiguo Tang, Xiaoteng Min and J. Cheng, "Thermal Management of a Cylindrical Lithium-Ion Battery Module Using a Multichannel Wavy Tube," *Journal of Energy Engineering*, vol. 145, pp. 246–267, 2019, (Accessed 2022-03-05).

[18] K. Ulrich and S. D. Eppinger, *Product Design and Development*. Tata McGraw-Hill Education, 2003.

[19] A2mac. Automotive benchmarking. [Online]. Available: https://portal.a2mac1.com (Accessed 2022-03-05).

[20] G. J, "Fast-Charging of Large Energy-optimised Li-ion Cells for Electrified Drivelines,Volvo Technology AB, BF68700,," *Energimyndigheten*, 2018.

A

Benchmarking

Table A.1: Benchmarking [19]

Benchmarked Product	Cell Format	Cell Level Solution	Cooling System	Nominal Capacity Rate
Nissan Leaf	Pouch	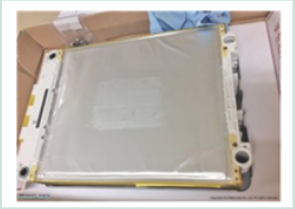 Radially Cooled	Passive Air-Cooled	1/3C – 1C
Polestar	Pouch	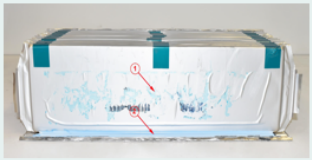 Long side Cooled	Active Liquid-Cooled	1C – 2.5C

DEPARTMENT OF MECHANICS AND MARITIME SCIENCES
CHALMERS UNIVERSITY OF TECHNOLOGY
Gothenburg, Sweden
www.chalmers.se

CHALMERS
UNIVERSITY OF TECHNOLOGY